

# A Simple Technique to Improve Contractile Effect of Cold Plasma Jet on Acute Mouse Wound by Dropping Water

メタデータ	言語: eng 出版者: 公開日: 2017-10-03 キーワード (Ja): キーワード (En): 作成者: メールアドレス: 所属:
URL	<a href="http://hdl.handle.net/2297/43924">http://hdl.handle.net/2297/43924</a>

# **A simple technique to improve contractile effect of cold plasma jet on acute mouse wound by dropping water**

Nasruddin<sup>1,2</sup>, Yukari Nakajima<sup>1</sup>, Kanae Mukai<sup>1</sup>, Emi Komatsu<sup>1</sup>, Heni Setyowati Esti Rahayu<sup>2</sup>,  
Muhammad Nur<sup>3</sup>, Tatsuo Ishijima<sup>4</sup>, Hiroshi Enomoto<sup>4,5</sup>, Yoshihiko Uesugi<sup>4,6</sup>, Junko Sugama<sup>7</sup>,  
Toshio Nakatani<sup>7</sup>

<sup>1</sup>Graduate Course of Nursing Science, Graduate School of Medical, Pharmaceutical and Health Sciences, Kanazawa University, Kanazawa-shi, Japan

<sup>2</sup>Faculty of Health Science, Muhammadiyah University of Magelang, 56172, Magelang, Central Java, Indonesia

<sup>3</sup>Department of Physics, Diponegoro University, Semarang, Indonesia

<sup>4</sup>Research Center for Sustainable Energy and Technology, Kanazawa University, Kanazawa-shi, Japan

<sup>5</sup>Faculty of Mechanical Engineering, Institute of Science and Engineering, Kanazawa University, Kanazawa-shi, Japan

<sup>6</sup>Faculty of Electrical and Computer Engineering, Institute of Science and Engineering, Kanazawa University, Kanazawa-shi, Japan

<sup>7</sup>Division of Nursing, Faculty of Health Sciences, Institute of Medical, Pharmaceutical and Health Sciences, Kanazawa University, Kanazawa-shi, Japan

**Corresponding author:**

Prof. Toshio Nakatani

Division of Nursing, Faculty of Health Sciences, Institute of Medical, Pharmaceutical and Health Sciences, Kanazawa University

5-11-80 Kodatsuno, Kanazawa-shi, Ishikawa-ken 920-0942, Japan

Tel.: +81 76 265 2542

Fax: +81 76 234 4363

Email: nakatosi@staff.kanazawa-u.ac.jp

**ABSTRACT**

A simple technique is tested to improve the contractile effect of a cold plasma jet on acute wounds of mice. Distilled water on the order of microliters is dropped onto wounds before treatment. To assess the fate of the water, an infrared thermal imager is applied. To evaluate the healing effect, macroscopic and immunohistological studies are conducted. Regarding the wound contractile effect, we show that combination treatment of plasma with dropped water seemed to have a greater effect than plasma treatment alone. Plasma may modify the wound surface through such water, chemically and physically. The histological stiffness of the wound surface during maturation and remodeling, however, may also influence the fate of the water during treatment.

## 1. Introduction

Collaborative efforts within the fields of plasma, biology and biomedical research to overcome obstacles around the application of cold atmospheric plasma treatment for wound care are part of the plasma medicine agenda <sup>[1] [2] [3]</sup>. It is well known that the flow rate of the carrier gas, such as Ar or He, can be used to reduce the temperature of an atmospheric plasma jet during its generation <sup>[4]</sup>; however, such gas may also contribute to the drying of a wound surface when it is the object of such treatment. According to modern perspectives on wound care, it has been suggested that normal wound healing should take place in a moist environment <sup>[5] [6]</sup>. It was also reported that the treatment of wounds with dry air can inhibit their healing due to evaporation <sup>[7] [8]</sup>.

In the plasma medicine community, it was established that the added value of cold plasma treatment may be associated with its possibility of producing biological molecules like reactive oxygen and nitrogen species (RONS) <sup>[9] [10]</sup>, which, at appropriate dosages, may promote wound repair <sup>[11] [12]</sup>. Accordingly, it is important to optimize the roles of RONS and to minimize the drying effect of cold plasma.

In both humans and animal models, wound contraction is a key event in the healing of full-thickness wounds <sup>[13]</sup>. It is well established that this process is influenced by the presence of myofibroblasts <sup>[14]</sup>. Referring to Hinz et al. <sup>[15]</sup>, there are multiple ways by which myofibroblasts originate, one of which is through their differentiation from fibroblasts. It has recently been shown that O<sub>2</sub> and ROS may trigger this mechanism <sup>[16]</sup>. On the basis of histological study of a mouse model mimicking a clinical setting, it was reported that daily treatment with a cold plasma jet for 1 minute on a full-thickness wound accelerated its healing through the promotion of wound contraction, among others <sup>[17]</sup>. In this previous study, wound size on day 7 in the cold

plasma-treated group was macroscopically significantly smaller than that in the control group, but there was no statistically significant difference regarding the mean myofibroblast count. Considering that wound healing is a complex living process consisting of orchestrated events communicated by collaborative biological substances <sup>[13]</sup> and that cold plasma may be able to intervene at the microenvironmental level <sup>[18]</sup>, it is not easy to identify and evaluate a single factor related to it. However, on the basis of macroscopic observation, it has been shown that the surface of the wound was drier after cold plasma treatment than that in a control <sup>[17]</sup>.

Against this background, the present study was conducted to evaluate a simple technique involving dropping water on the order of microliters that attempts to reduce the drying effect during cold plasma treatment on the wound surface. We used a mouse model mimicking a clinical setting and employed water because it was reported that water is commonly used in the community and in hospitals for cleaning wounds due to its accessibility, efficiency and cost-effectiveness <sup>[19]</sup>. We hope that this research bridges the gap between cellular- and human-level studies in plasma medicine for community and hospital settings.

## **2. Experimental**

### **2.1. Cold plasma jet system**

This research used a cold atmospheric pressure plasma jet system provided by the Division of Electrical Engineering and Computer Science, Kanazawa University, Kanazawa, Japan, as shown in **Figure 1**. This device was developed based on the work of Teschke *et al.* <sup>[20]</sup>. In order to enable comparison with our previous results <sup>[17]</sup>, Ar gas was chosen as the carrier gas for the cold atmospheric pressure plasma jet. Two metal ring electrodes were used around the quartz

tube for this system. It had a quartz tube with a 1.6 mm inner diameter and 3.0 mm outer diameter. The distance between the two electrodes was 1 mm. The lower ring electrode was connected to the ground. A low-frequency ( $\sim 20$  kHz) AC high voltage, with a peak-to-peak voltage of 25 kV, was applied to the upper ring electrode when Ar gas (99.995% purity) at a flow rate of 5 standard liters per minute (slm) was injected from one end of the quartz tube. A high-voltage probe (P6015A; Tektronix, Inc., Tokyo, Japan) and a current probe (8585C; Pearson Electronics, Palo Alto, CA, USA) were applied to measure the discharge voltage and discharge current to estimate the amount of power consumed by the power supply. The average power density at the electrode was  $85 \text{ W/cm}^2$ .

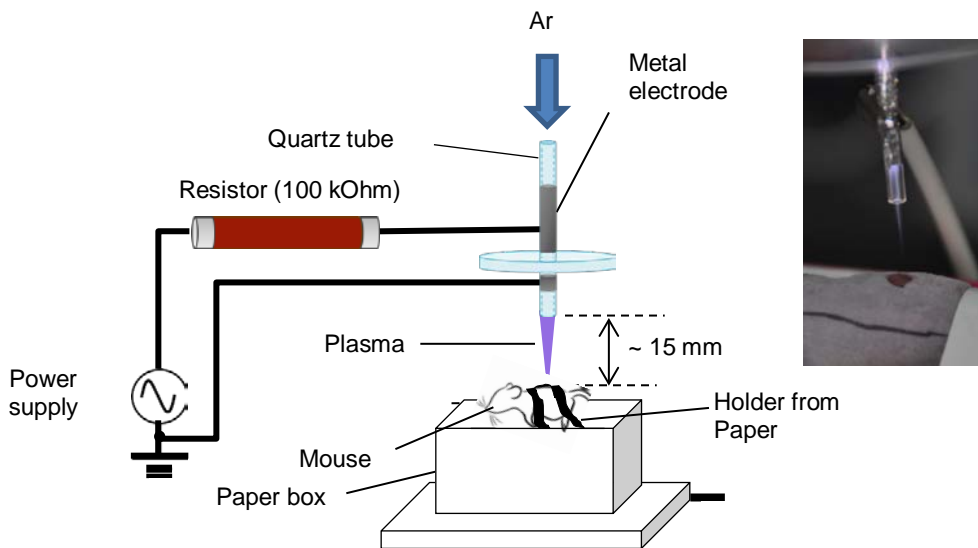


**Figure 1\_**Experimental set-up. *Digital image:* wound during plasma treatment

## 2.2. Thermal and safety evaluation of cold plasma jet on normal skin

### a. Nozzle tip–skin surface distances versus $\Delta T$

The hair of three BALB/c mice under anesthetized conditions was shaved one day before the experiment. Under anesthetized conditions, they were then treated with a cold plasma jet under the following conditions:  $\text{Ar}$  gas flow rate = 5 slm; peak-to-peak voltage = 25 kV; nozzle tip–skin distances ( $d$ ) = 5, 10 and 15 mm; and treatment time = 2 minutes. The dorsal skin of each mouse was treated with different spots, so that there were 4 spot samples in every experimental mouse. A digital camera (LUMIX DMC-FX07) was used to document the experimental conditions, during and after treatment. During treatment, the temperature distribution of treated skin and its surroundings was measured using a non-contact infrared digital camera (IR camera) (F30S; NEC Avio Infrared Technologies, Tokyo, Japan). Using this camera, about ten images were taken for each sample during 2 minutes. After treatment, the skin was observed visually.

The relationship between nozzle tip–skin surface distance and  $\Delta T$  was evaluated.  $\Delta T$  was calculated as  $T_p - T_{ni}$ , in which  $T_p$  is the peak temperature spot of skin under plasma treatment and  $T_{ni}$  is the temperature spot on skin with no plasma treatment.  $T_p$  and  $T_{ni}$  were obtained from a thermal image processed using InfReC Analyzer NS9500 Lite. Finally, ANOVA was applied to analyze the differences between group means.

### b. Flow rate of $\text{Ar}$ gas versus $\Delta T$

Under the aforementioned conditions of experimental mice, those of a cold plasma jet and those of a procedure with minor modification were applied in this section. Four mice were used. The nozzle tip–skin surface distance ( $d$ ) was fixed at 15 mm and the flow rates of  $\text{Ar}$  gas

were varied among 2, 3, 4 and 5 slm. The dorsal skin of each mouse was treated with different spots, so that there were 4 spot samples in every experimental mouse. The relationship between the flow rate of Ar and  $\Delta T$  was evaluated as described previously.

### **2.3. Evaluation of OH radical, H<sub>2</sub>O<sub>2</sub> and NO<sub>3</sub><sup>-</sup> generation in the liquid phase**

OH radical generation in liquid was evaluated using terephthalic acid (TA, Nacalai Tesque), as applied previously<sup>[21]</sup>. Terephthalic acid reacts with OH radicals to generate 2-hydroxyterephthalic acid (HTA) with stable fluorescence<sup>[22][23]</sup>. Specifically, a plastic vessel containing 1.2 ml of 3 mM TA solution in NaOH aqueous solution (7.5 mM) and without cells was treated with a plasma jet under the following conditions: Ar gas flow rate = 5 slm; peak-to-peak voltage = 25 kV; nozzle tip–solution surface distance = 10, 15 and 20 mm; and treatment time = 60, 180, 300 and 420 s/vessel. HTA fluorescent signals generated by the reaction of TA with OH radicals were detected with a microplate spectrofluorometer (Gemini XPS, Molecular Devices, Sunnyvale, CA, USA) at excitation and emission wavelengths of 315 nm and 425 nm, respectively. Using an authentic HTA external standard, the fluorescent signals were converted to concentrations. A calibration curve over the range of 0.5-100  $\mu$ M was generated by making a series of 2HTA dilutions in NaOH solution.

H<sub>2</sub>O<sub>2</sub> was evaluated using ultrapure water. Ultrapure water in a cuvette was treated with a plasma jet under the same conditions with modification of the treatment time in the range of 20-120 s. H<sub>2</sub>O<sub>2</sub> in the ultra-pure water medium was analyzed by a peroxidase enzyme method using a commercially available reagent (Kyoritsu Chemical-Check Lab., Model WAK-H2O2, range: 0.05-5.0 mg/L) immediately after cold plasma treatment. This method was also previously

applied by other researchers <sup>[24]</sup>. The concentration of H<sub>2</sub>O<sub>2</sub> was determined with a UV-vis absorption spectrometer (Hitachi, U-2810) using the absorption peak at 540 nm.

The conditions of cold plasma treatment for the evaluation of nitrogen-based species, NO<sub>3</sub><sup>-</sup>, resembled those for H<sub>2</sub>O<sub>2</sub>. The treatment times of plasma were varied among 60, 180, 300 and 420 s. The presence of such species in water was detected using ion chromatography performed using the Shimadzu Prominence HPLC system with IC-SA2, for an anion separation column, and IC-C4, for a cation separation column.

#### **2.4. Animals and experimental protocol**

Forty-eight BALB/c CrSlc male mice aged 8 weeks (Sankyo Lab Service Corporation, Inc., Toyama, Japan) and weighing 21.3–26.0 g were used. They were caged individually in an air-conditioned room at 25.0 ± 2.0 °C with light from 08:45 to 20:45 h and under *ad libitum* feeding conditions. All of the animal experiments conducted in this study were reviewed and approved by Kanazawa University Animal Experiment Committee and the experimental protocol and animal care followed the Guidelines for the Care and Use of Laboratory Animals of Kanazawa University, Japan (AP: 112243).

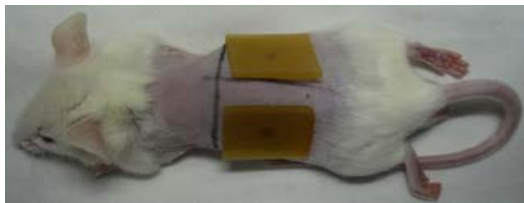
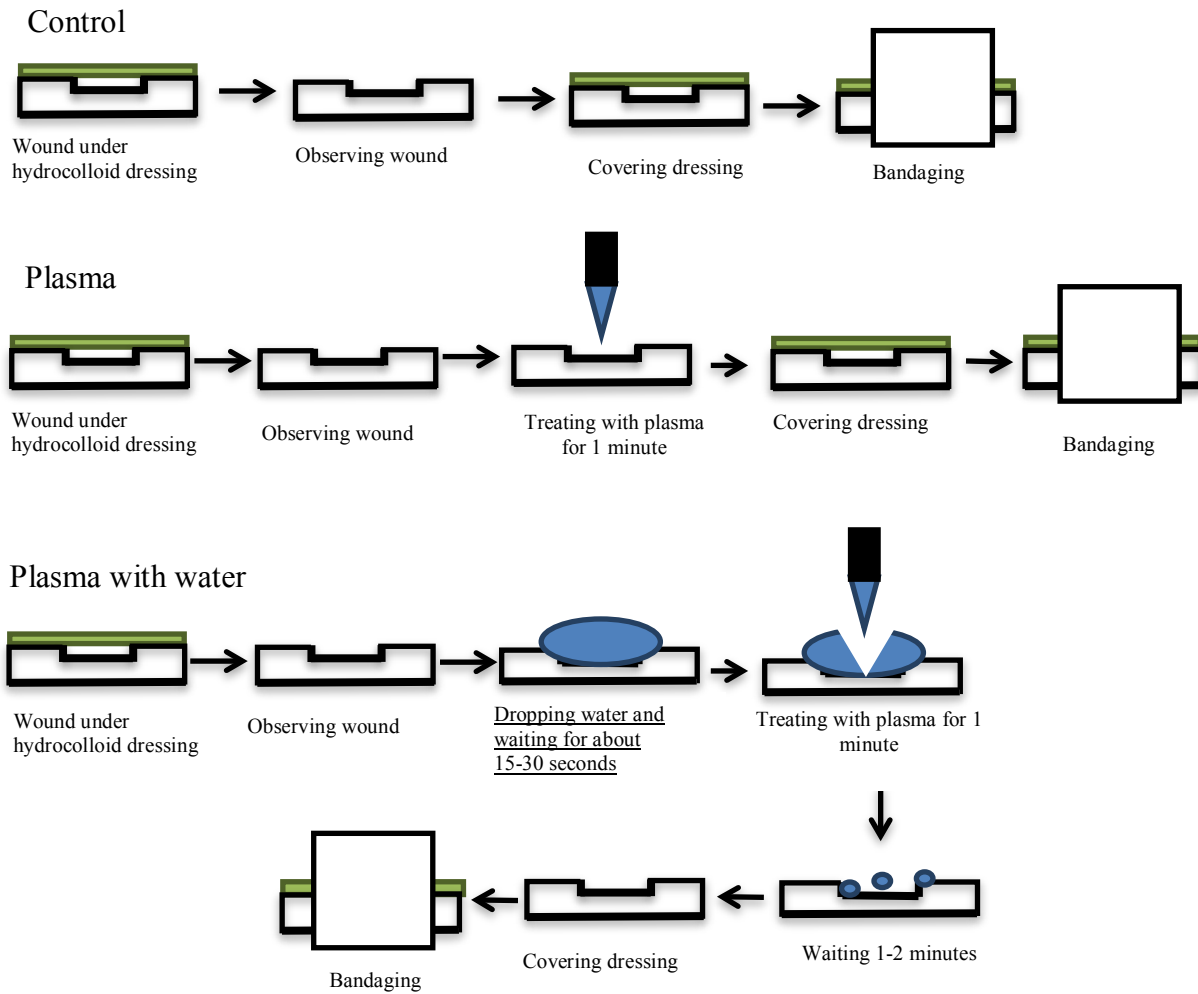
#### **2.5. Wound healing model and plasma treatment**

A full-thickness wound with a diameter of 4 mm was created on dorsal skin of a mouse using a punch biopsy of 4 mm following a previously described procedure <sup>[17]</sup>. Plasma treatment was conducted once daily for 1 minute in one spot at the center of the wound. The position of the wound surface was about 15 mm under the nozzle tip, as shown in **Figure 1**. Room temperature during the experiment was 21-24 °C.

The experimental procedure after day 0 is shown in **Figure 2**. Generally, the mice were randomly classified into three groups:

- a. Control group (C): Wounds were allowed to heal daily under hydrocolloid dressing (Tegaderm; 3M Health Care, Tokyo, Japan) to maintain their moist environment. To maintain hydrocolloid dressing coverage of the wound, the mouse body was then bandaged.
- b. Group with plasma treatment only (P): Wounds were treated with a cold plasma jet for 1 minute and then covered with hydrocolloid dressing. To maintain hydrocolloid dressing coverage of the wound, the mouse body was then bandaged.
- c. Group with combination treatment of plasma with dropped water (PW): Wounds were subjected daily to the dropping of 40  $\mu$ L of distilled water and treated using a cold plasma jet for 1 minute, after which about 1-2 minutes was allowed to pass before they were covered with hydrocolloid dressing. To maintain hydrocolloid dressing coverage of the wound, the mouse body was then bandaged.

A



B



C

**Figure 2.** A. Experimental procedure. B. Wound under hydrocolloid dressing. C. Bandaged mouse.

## **2.6. Evaluation of the fate of dropped water during cold plasma treatment**

We assumed that dropped water and wound fluid may contribute to support the healing effect of cold plasma treatment by establishing a beneficial environment in the wound. To achieve such conditions, the presence of water on the surface of the wound during the treatment was a prerequisite. Considering that (a) a cold plasma jet has a gas flow that may affect both dropped water and the wound surface, and (b) the wound experiences histological maturation during its healing, we hypothesized that the meeting of the cold plasma jet and the dropped water on the wound may collaborate to produce a defined pattern in the period of observation.

In order to test this hypothesis, the conditions were classified into two experimental results: (a) conditions with a defined pattern, if the wound area and its surroundings were mostly covered with water; and (b) conditions with no defined pattern, if the conditions in (a) were not exhibited. To monitor these conditions, a non-contact infrared camera (F30S; NEC Avio Infrared Technology, Tokyo, Japan) was applied. This camera was employed at a distance of about 15 cm from the object. Using it, approximately 8 images were obtained for every sample from day 1 until day 11. InfRec Analyzer NS9500 Lite was applied to process such images. Comparative study of the obtained images was conducted from day to day during the observation period.

## **2.7. Macroscopic evaluation**

The day when wounds were made was designated as day 0, and the process of wound healing was observed daily from day 0 to day 14 after wounding. Before observation, the environment surrounding the wounds was cleaned with saline solution. Wound edges were traced on polypropylene sheets and photographs were taken every day. The traces on the sheets were captured with a scanner onto a personal computer using Adobe Photoshop Elements 7.0

(Adobe System Inc., Tokyo, Japan), and the areas of the wounds were calculated using the image analysis software Scion Image Beta 4.02 (Scion Corporation, Frederick, Maryland, USA).

## **2.8. Prediction of healing day**

The day of wound healing was predicted based on a graph of the ratio of wound area to initial wound area. Initially, the overall trend of this graph was evaluated. Wound healing day was plotted on the y-axis when the trend of reduction of wound size started to become flat, as reported previously<sup>[17]</sup>, which was at 0.3 (see **Figure 6a**). At that point, it was assumed that new epithelium completely covered the wound surface in all samples for all groups. From that plotted point, line z was made, crossing the lines of reduction for every group. Wound healing days at points  $\hat{p}_w$ ,  $\hat{p}$  and  $\hat{c}$  were further created based on the lines from their meeting points to the x-axis.

## **2.9. Tissue processing**

The mice were euthanized by a massive pentobarbital sodium IP injection on day 7, 11 or 14 post-wounding. The wounds and the surrounding normal skin were excised, stapled onto polypropylene and fixed in neutral buffered 10% formalin solution in 0.01 M phosphate buffer, at pH 7.4, for about 15 hours. The samples were then rinsed in 0.01 M phosphate-buffered saline (PBS) for about 8 hours. Subsequently, they were dehydrated in an alcohol series, cleaned in xylene and embedded in paraffin to prepare serial 5- $\mu$ m sections.

Immunohistochemical staining for myofibroblasts was conducted in line with our procedure as reported previously<sup>[17]</sup>. The tissue sections were incubated with primary antibody, anti- $\alpha$ -smooth muscle actin (anti- $\alpha$ -SMA) (Abcam Japan, Tokyo, Japan) (1:100 in Tween-PBS),

at 4 °C overnight, and then with secondary antibody, Dako EnVision+System-HRP Labeled Polymer Anti-Mouse (Dako North America Inc., CA), at room temperature for 30 minutes. After completion of the incubation with the secondary antibody, the sections were reacted with 3,3'-diaminobenzidine substrate (Dako ENVISION Kit/HRP (DAB), Dako Japan, Kyoto, Japan) for staining for about 2-5 minutes at room temperature. Finally, counterstaining was conducted using hematoxylin.

### **2.10. Microscopic observations**

On the basis of the anti- $\alpha$ -SMA staining result using an Olympus BX50 light microscope (Olympus, Tokyo, Japan) at a magnification of 400x, myofibroblasts were counted. Using an Olympus DP72 digital camera and Olympus DP2-BSW software, images were captured. Three squares were selected at each wound margin and the center of the wound, on four serial sections per wound. The data are presented as the mean number of stained cells counted in the twelve squares; four serial wound sections per wound were analyzed.

### **2.11. Statistical analysis**

Data were subjected to statistical analyses using SPSS 16.0. Mean differences between the PW, P and control groups for  $\Delta T$ , the ratio of average wound area to the original wound area, the number of days of wound healing and the results of myofibroblast counts were evaluated by ANOVA followed by the Tukey-Kramer method; p-values <0.05 were considered significant.

### 3. Results

#### 3.1. Thermal and safety evaluation of cold plasma jet on normal skin

TABLE 1. Representative examples of skin condition images used to evaluate the thermal and safety effects of plasma treatment as a function of nozzle tip-skin distance ( $d$ ). Histogram shows the relationship between  $d$  and  $\Delta T$ .

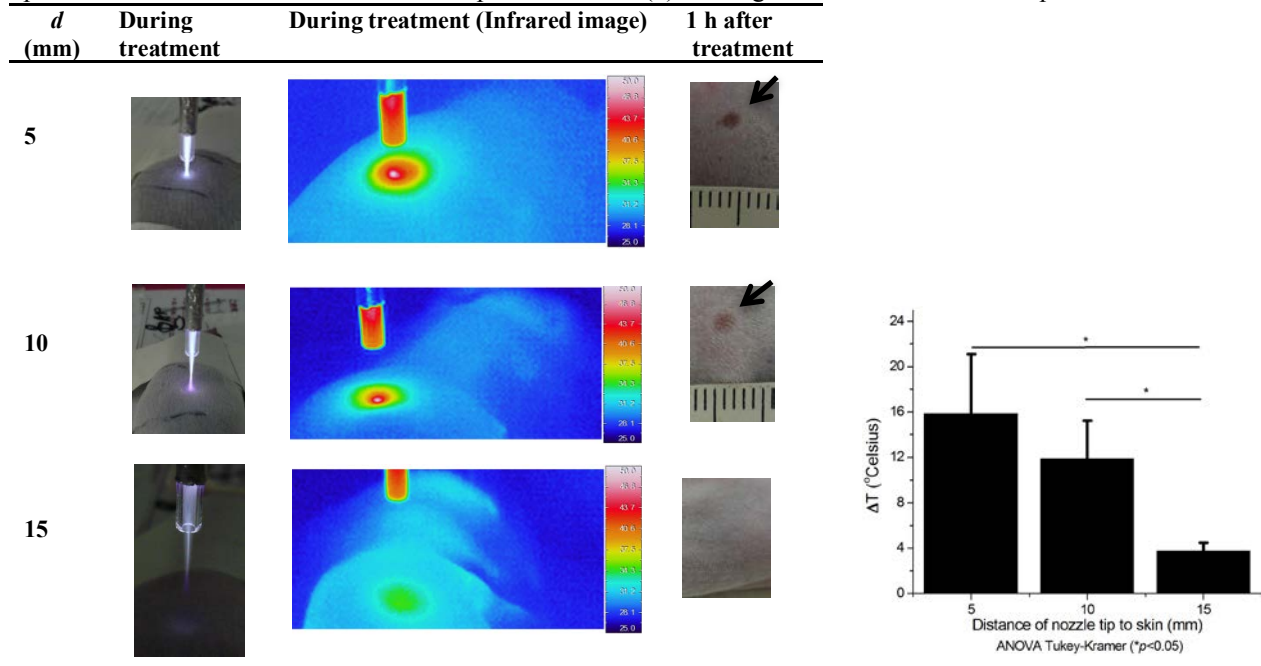
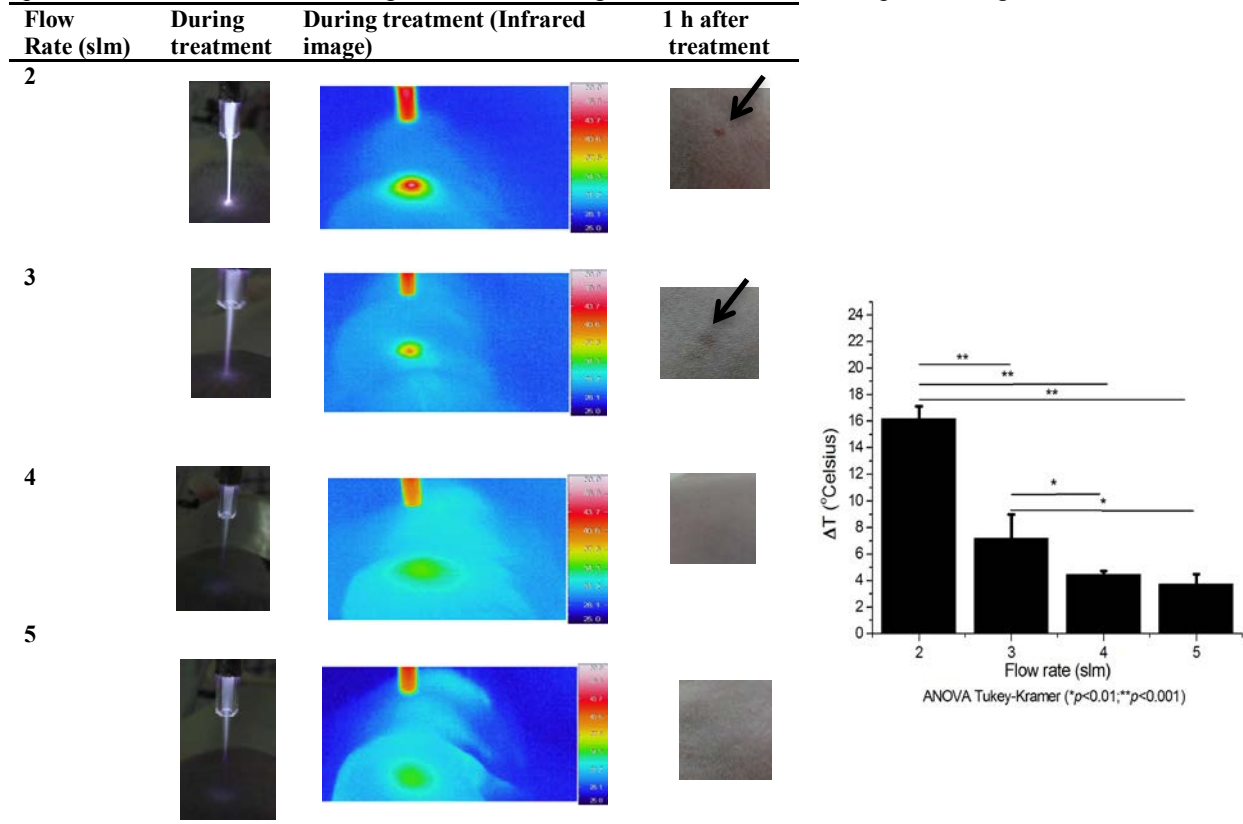


TABLE 2. Representative examples of skin condition images used to evaluate the thermal and safety effects of plasma treatment as a function of gas flow rate. Histogram shows the relationship between gas flow rate and  $\Delta T$ .



*a. Nozzle tip–skin surface distances versus  $\Delta T$*

A uniform temperature distribution on skin under plasma treatment at 15 mm was observed with a temperature of about 34 °C (green band). In contrast, a non-uniform temperature distribution on skin under plasma treatment at 5 and 10 mm was observed with peak temperatures at their centers reaching between 48 and 50 °C (white band). Unfortunately, injury was observed about 1 hour after plasma treatment at 5 and 10 mm, whilst this was not observed at 15 mm (**Table 1**). Additionally, plasma treatment with nozzle–skin distances of 5 mm, 10 mm and 15 mm caused  $\Delta T$  (elevated skin temperature) of  $16 \pm 5^\circ\text{C}$ ,  $12 \pm 3^\circ\text{C}$  and  $4 \pm 1^\circ\text{C}$ , respectively.  $\Delta T$  at 15 mm was significantly lower than those at 5 mm and 10 mm.

*b. Flow rate of Ar gas versus  $\Delta T$*

A uniform temperature distribution on skin under plasma treatment at 4 and 5 slm was observed with a temperature of about 34 °C (green band). In contrast, a nonuniform temperature distribution on skin under plasma treatment at 2 and 3 slm was observed with peak temperatures at the centers that reached between 48 and 50 °C (white band) and 42 and 44 °C (red band). Unfortunately, abnormal skin was observed about 1 hour after plasma treatment with gas flow rates of 2 and 3 slm, whilst this was not observed at 4 and 5 slm. Additionally, plasma treatment with gas flow rates of 2, 3, 4 and 5 slm caused elevations of skin temperature of  $16 \pm 1^\circ\text{C}$ ,  $7 \pm 2^\circ\text{C}$ ,  $4 \pm 0.5^\circ\text{C}$  and  $4 \pm 1^\circ\text{C}$ , respectively (**Table 2**).  $\Delta T$  at 5 slm was significantly lower than those at 2 slm and 3 slm, but was not significantly lower than that at 4 slm.

### 3.2. Evaluation of OH radical, H<sub>2</sub>O<sub>2</sub> and NO<sub>3</sub><sup>-</sup> generation in the liquid phase

Both the amounts and the generation rates of HTA, H<sub>2</sub>O<sub>2</sub> and NO<sub>3</sub><sup>-</sup> were calculated and plotted on graphs. The generation rates of HTA, H<sub>2</sub>O<sub>2</sub> and NO<sub>3</sub><sup>-</sup> were calculated from the total amounts of these chemicals produced in plasma-treated liquid, as shown in **Figures 3a, 3b** and **3c**, respectively, assuming that the amounts of these chemicals increase linearly with increasing plasma treatment time. The amounts of HTA, H<sub>2</sub>O<sub>2</sub> and NO<sub>3</sub><sup>-</sup> decreased with increasing nozzle tip–liquid surface distance, but they increased with increasing treatment time. The generation rates of HTA, H<sub>2</sub>O<sub>2</sub> and NO<sub>3</sub><sup>-</sup> were relatively constant even when the applied distances were changed. In the present study, a generation rate of H<sub>2</sub>O<sub>2</sub> of approximately 2 nmol/sec was detected at an applied distance of 15 mm.

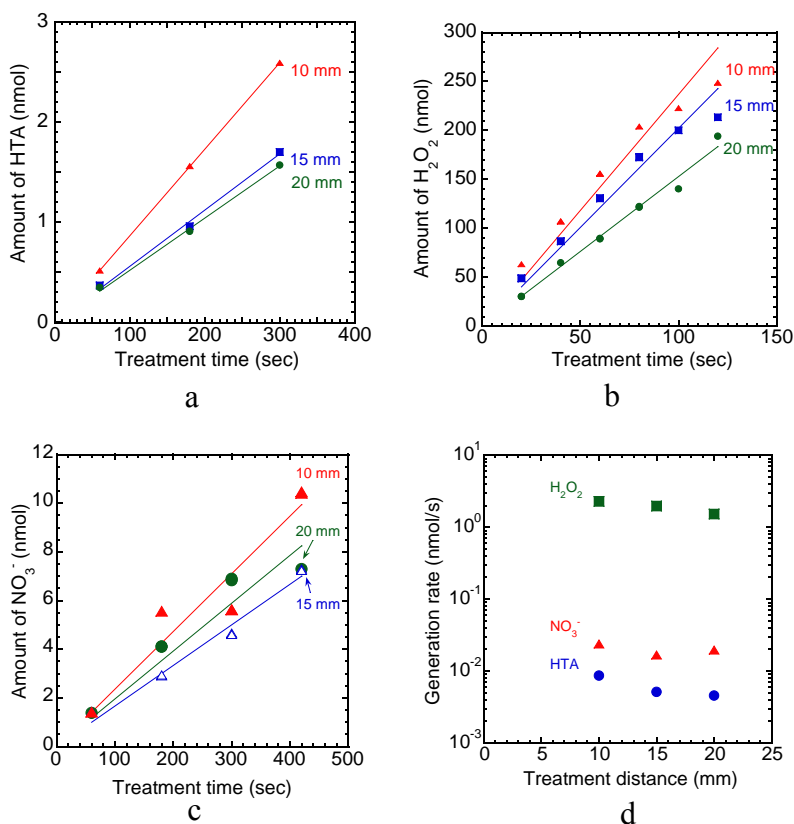


**Figure 3.** a. Amount of HTA. b. Amount of H<sub>2</sub>O<sub>2</sub>. c. Amount of NO<sub>3</sub><sup>-</sup>. d. Generation rates of HTA, H<sub>2</sub>O<sub>2</sub> and NO<sub>3</sub><sup>-</sup> at treatment distances of 10, 15 and 20 mm.

### 3.3. Evaluation of the fate of dropped water during plasma treatment

Evaluation of the fate of the water dropped on the wounds under plasma treatment was conducted from day 1 to day 10. In infrared thermal images, the presence of water or that of liquid was represented by a blue color. During the 10 days of observation, there was variation in the appearance of the water dropped on the wounds. From day 1 to day 3, a defined pattern with a blue color, as shown in **Figure 4 (day 1)**, was observed in all samples of PW. This appearance showed that the surroundings of the wound surface were consistently covered with water. Considering digital and infrared images, it seemed likely that, under plasma treatment, at first, the water surface was suppressed by the blowing of Ar gas. Consequently, it moved down and was concentrated along the edge of the wound and on the surrounding skin. From day 4 to day 7, however, the number of samples with this pattern decreased gradually. Finally, on days 9 and 10, no defined pattern was observed. On these two days, water left the wound surface and its surroundings during treatment, as shown in **Figure 4 (day 9)**.

In samples of P, a blue color was also observed in a smaller round area during the inflammation phase. This represented natural inflammation fluid. On the other hand, on days 9 and 10, it appeared that the condition of plasma influenced the area of PW and that of P relatively similarly. Skin under plasma was slightly elevated. There was an area with a slightly elevated temperature under plasma treatment, which the plasma seemed to have warmed.

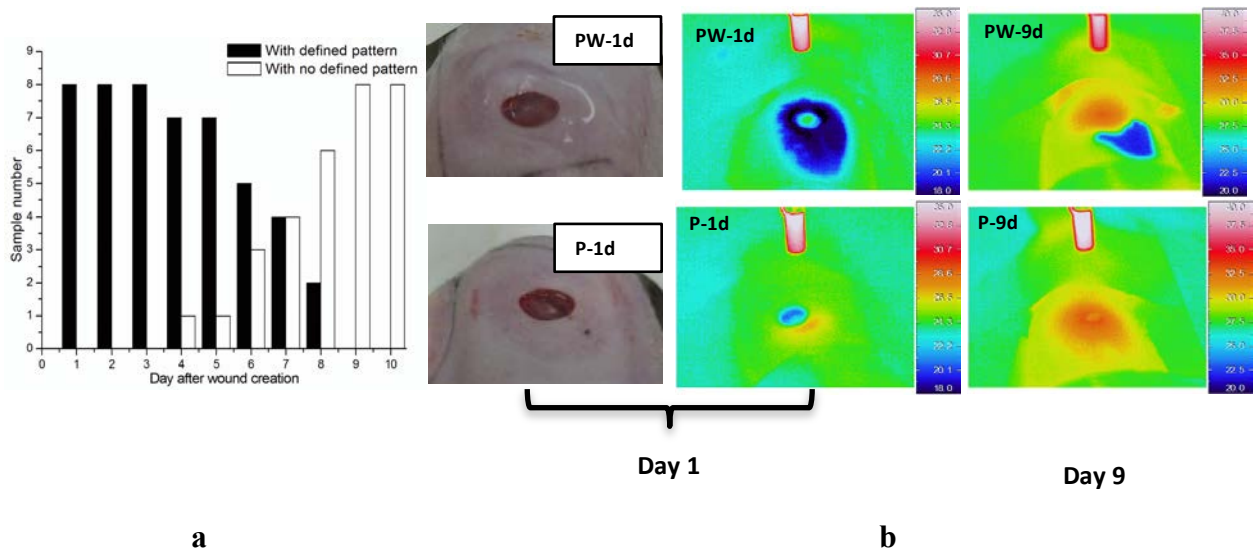


**Figure 4.** a. Histogram showing the number of samples in PW with a defined pattern and no defined pattern from day 1 to day 10. b. Representative appearances of digital images and those of infrared thermal images during cold plasma treatment with a defined pattern (PW-1d) and with no defined pattern (PW-9d). Inflammation fluid colored blue is exhibited in P-1d. Abbreviations: PW-1d: sample image of PW at day 1; P-1d: sample image of P at day 1; PW-9d: sample image of PW at day 9; P-9d: sample image of P at day 9.

### 3.4. Macroscopic observation

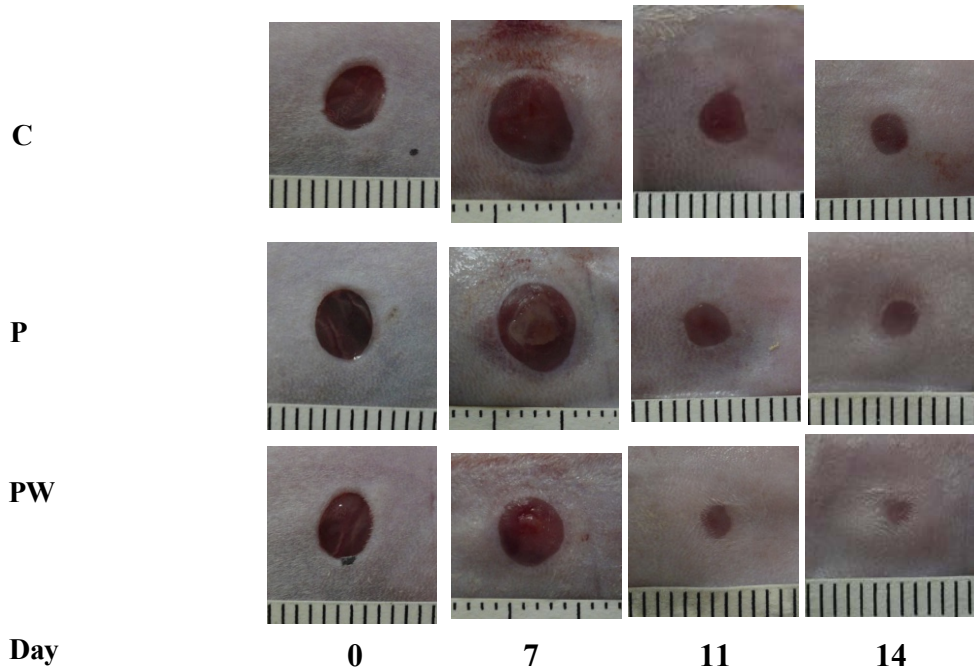


**Figure 5.** Macroscopic observation of wound healing.

Wounds in all groups were observed from day 0 to day 14, as shown in **Figure 5**. From day 1 to day 5, wounds in all groups expanded due to edema and then gradually decreased in size until the end of this period. From day 7 to day 14, wounds in PW were smaller than in P and C. There were no marked differences regarding the condition of the wound surface among C, P and PW. During the inflammation stage, from day 1 until approximately day 6, exudate appeared in all groups. From day 7 to day 14, the wound surfaces in all groups were mostly fresh.

### 3.5. Wound area reduction and day of wound healing

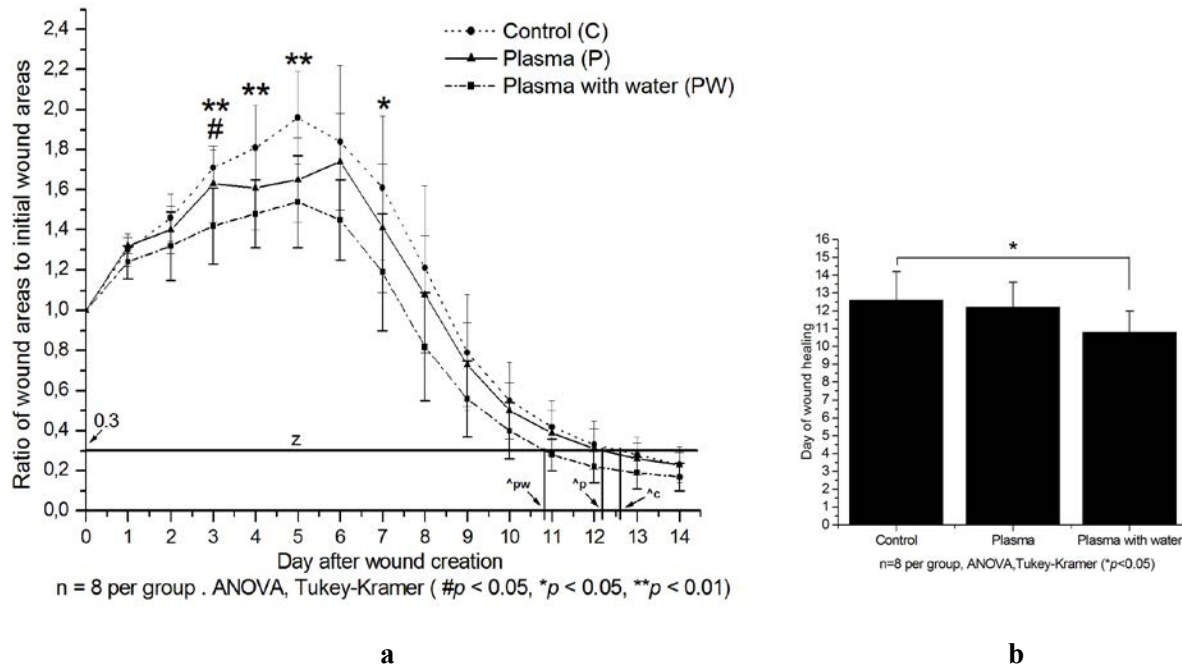


**Figure 6. a.** Ratio of wound areas to initial wound areas during healing. Note that: (i) # shows significance level of P to C, while \* and \*\* show that of PW to C; (ii) points  $\wedge_{pw}$ ,  $\wedge_p$  and  $\wedge_c$  show days of wound healing prediction for PW, P and C, respectively; **b.** Histogram regarding days of wound healing prediction for every group. Days of wound healing prediction for C, P and PW were  $12.6 \pm 1.6$ ,  $12.2 \pm 1.4$  and  $10.8 \pm 1.2$  days, respectively.

Generally, there were similar patterns with respect to wound area reduction in all groups, as shown in **Figure 6a**. They expanded from day 0 to day 5 or 6, and then gradually decreased in size from day 6 or 7 until the end of the observation period. On observation at days 4-8, all wounds in P were smaller than those in C, but P and C means were not significantly different (days 4-8:  $P > 0.05$ ). On the other hand, in this period, on days 3, 4, 5 and 7, all wounds in PW

were smaller than those in C, in which PW and C means were significantly different (day 4:  $P < 0.01$ ; day 5:  $P < 0.01$ ; day 7:  $P < 0.05$ ). Additionally, in the same observation period, all wounds in PW were smaller than those in P, but PW and P means were not significantly different (days 4-8:  $P > 0.05$ ). At the end of the observation period, there were no statistically significant differences between PW and C, or between PW and P; however, the wound size of PW was the smallest.

Days of wound healing for C, P and PW were  $12.6 \pm 1.6$ ,  $12.2 \pm 1.4$  and  $10.8 \pm 1.2$  days, respectively, as shown in **Figure 6b**. The day of wound healing for PW was significantly earlier, by about 2 days, than that for C ( $P < 0.05$ ). On the other hand, the day of wound healing for P was earlier than that for C, but the two means were not significantly different ( $P > 0.05$ ).

### 3.6. Myofibroblast count

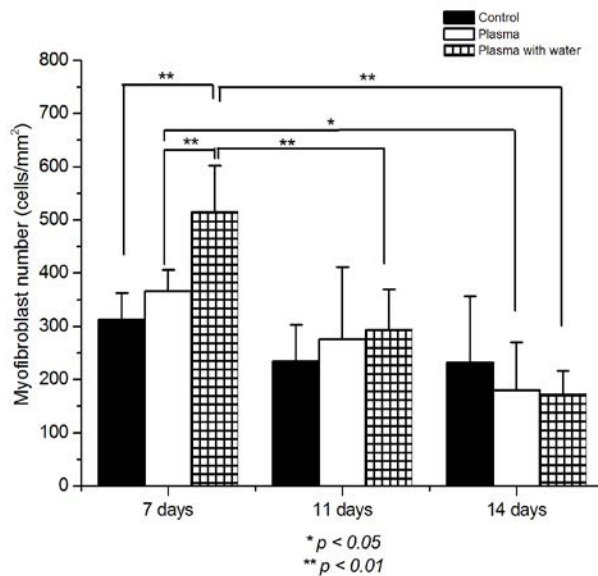


**Figure 7.** Histogram of myofibroblast number on days 7, 11 and 14. By day 7, myofibroblast number in the PW group was significantly greater than those in C and P.

Myofibroblasts on days 7, 11 and 14 were calculated (**Figure 7**). The numbers of myofibroblasts per mm<sup>2</sup> in PW and P peaked on day 7 and then decreased gradually until day 14, while that in C also peaked on day 7, decreased on day 11 and then tended to be stable on day 14. On day 7, the number of myofibroblasts in PW was significantly greater than those in P ( $P<0.01$ ) and C ( $P<0.01$ ), while that in P was greater than that in C, but P and C means were not significantly different ( $P>0.05$ ). On day 11, the number of myofibroblasts in PW was greater than those in P and C, but the two means were not significantly different (PW vs. P:  $P>0.05$ ; PW vs. C:  $P>0.05$ ). On the other hand, on day 14, the number of myofibroblasts in PW was lower than those in P and C, but the means were not significantly different (PW vs. P:  $P>0.05$ ; PW vs. C:  $P>0.05$ ). On day 14, the numbers of myofibroblasts in PW, P and C were lower than those on day 7. The two means in the first and second groups were significantly different (PW:  $P<0.01$ ; P:  $P<0.05$ ), but those in the latter two groups were not ( $P>0.05$ ).

#### **4. Discussion**

In this study, we show that combination treatment of dropping water with plasma provided an improvement over just plasma treatment for the healing of full-thickness acute wounds on mouse skin. It has been established that wound healing consists of three main phases: inflammation, granulation tissue formation and matrix formation/remodeling<sup>[13]</sup>. In this study, on days 4-8 or from the late stage of the inflammation phase until the granulation phase of wound healing: (a) the wound size in the plasma-treated group was not significantly smaller than that in the control group; and (b) wound size on days 4, 5 and 7 in the combination-treated group was significantly smaller than that in the control group. Thus, it was suggested that combination treatment of dropping water with plasma caused a greater reduction of wound size than plasma treatment alone during this phase. Secondly, considering that, on day 7, myofibroblast count in

the plasma-treated group was significantly higher than that in the control, while that in the combination-treated group was significantly higher than those in the plasma-treated and control groups, it was indicated that combination treatment of plasma with dropped water was most effective to promote myofibroblasts. This indicates that there is a strong correlation between the reduction of wound size and increased myofibroblast count. Finally, in terms of the effectiveness of promoting wound contraction, combination treatment of plasma with the dropping of water seemed to have a greater effect than plasma treatment alone.

The greater effectiveness of combination treatment for wound contraction may be correlated with the presence of a defined pattern of dropped water during plasma treatment, as shown in the infrared thermal images. This appearance, however, was only observed on certain days. Considering that wounds were treated under the same plasma source conditions, it was suggested that this appearance may represent the histological phenomena of the wound surface during its healing. It is well established that the wound matrix experiences maturation. In early wound healing, it is thin, and then during maturation and remodeling, when the matrix becomes denser with thicker, stronger collagen fibrils, it becomes stiff in order to support isometric tension of the wound <sup>[25]</sup>. Under gas-blowing conditions, water dropped on a thin surface of a wound was partly trapped, while all of the dropped water on the stiff surface of a wound tended to leave it. This may explain why the defined pattern of dropped water was observed in all samples during the inflammation phase, from day 1 to 3, while it was not observed on days 9 and 10. Interestingly, days 4-8 seemed to represent a transition period, with the samples in this period being varied.

This research identified the presence of H<sub>2</sub>O<sub>2</sub> and nitrogen-based species at the applied distance (15 mm under the nozzle of the plasma reactor). Additionally, using an infrared thermal

imager, an area with a slightly elevated temperature on the wound under the influence of plasma was detected. Referring to Xia et al. <sup>[26]</sup>, it was reported that radiative warming stimulated the growth of wound-related cells, namely, fibroblasts.

In this experiment, in terms of the flow rate of Ar gas, it was applied at 5 slm and mouse wounds were positioned about 15 mm under the nozzle tip of the plasma reactor. These conditions were adopted after considering the thermal and safety effects of a plasma jet on normal mouse skin on the basis of two relationships: nozzle tip–skin surface distance versus  $\Delta T$  and flow rate of Ar gas versus  $\Delta T$ , as shown in **Tables 1** and **2**. Of course, the gas flow rate in this experiment was higher than in other studies reported previously <sup>[27]</sup> <sup>[28]</sup> <sup>[29]</sup>. Under its influence, the wound surface with a defined pattern was split into two defined areas: (1) along the edge of the wound, it was associated with concentrated water; and (2) partly in the center of the wound, it was covered with a low level of or no water, with it being difficult to distinguish exactly between these two options because of the presence of natural inflammation liquid. Regarding the former condition, water may have two main actions: (1) to reduce the evaporative area; and (2) to enhance chemically and control physically H<sub>2</sub>O<sub>2</sub> and nitrogen-based species of wounds. Regarding the latter condition, in the case of wounds covered with water, even at a low level, the aforementioned conditions may develop. Conversely, in the case of a wound surface with no water, the wound surface would directly interact with the reactive species of plasma jet. Consequently, radiative warming and such reactive species in the gas phase, RONS, may become key players and evaporation may occur.

A possible mechanism for the cold plasma to support wound healing was discussed previously <sup>[17]</sup>. Regarding the contractile effect on wounds, it was stated that plasma may take part in the differentiation from fibroblasts to myofibroblasts through promoting fibroblast

proliferation and/or activating transforming growth factor beta (TGF- $\beta$ ). In this context, dropping water may not produce a new pathway, but may support this existing pathway through enhancing the production of H<sub>2</sub>O<sub>2</sub> and minimizing the evaporative environment of the wound surface.

Generally, it is well understood that H<sub>2</sub>O<sub>2</sub> has negative and positive effects on chronic and acute wounds. At relatively high doses, it can not only kill bacteria but also damage healthy normal tissue <sup>[30]</sup>. Referring to Roy et al.<sup>[31]</sup>, however, it was reported that topical treatment of H<sub>2</sub>O<sub>2</sub> at a micromolar concentration could improve the healing of acute wounds. Accordingly, in the sense of the wound contractile effect, the generation rate of H<sub>2</sub>O<sub>2</sub> of about 2 nmol/s during 1 minute under the conditions applied in this study may macroscopically reflect the latter, but regarding the involved method, there are three significant differences:

- (a) Roy et al. applied relatively pure H<sub>2</sub>O<sub>2</sub>, but plasma-generated H<sub>2</sub>O<sub>2</sub> within water together with other substances, like NO<sub>3</sub><sup>-</sup>, was also detected in this experiment. Thus, the synergy of H<sub>2</sub>O<sub>2</sub> and such species could contribute to healing.
- (b) In the work of Roy et al., H<sub>2</sub>O<sub>2</sub> was formulated *before* the treatment and applied under steady state conditions, but in this study, it was generated *during* treatment and under the influence of plasma. In particular, the flow of gas influenced the distribution area of water containing H<sub>2</sub>O<sub>2</sub> and NO<sub>3</sub><sup>-</sup> on the wound surface.
- (c) Cold plasma jet in this experiment also produced warmth. Referring to Xia et al. <sup>[26]</sup>, it was reported that radiative warming stimulated the growth of wound-related cells, namely, fibroblasts.

A wide range of methods to control the effect of plasma treatment for safe medical applications have received a lot of attention. A number of plasma sources have also been developed. In addition, variation in the duration of plasma exposure was applied. Single or multiple gas ingredients of plasma were also explored. At the same time, cellular, ex vivo and in vivo models have been applied to evaluate related biological effects. To the best of our knowledge, however, this is the first report regarding how to select cold plasma treatment based on thermal and safety effects on normal mouse skin using a non-contact infrared thermal camera. This is also the first report regarding how to control the effect of plasma treatment through modifying the surface of the target using water in an in vivo model. However, there are several limitations in this research. The parameters of the wound surface, like pH, were not monitored, and also conditions like room temperature and room humidity were not controlled. Finally, the results of histological evaluation should also be clarified by molecular or cellular studies. These issues are topics for future investigations.

## **5. Conclusion**

It was observed that a simple technique using combination treatment of cold plasma jet with dropped water provided an improvement over just plasma treatment in terms of accelerating the healing of a full-thickness acute wound on mouse skin. This technique improved wound contraction during the late stage of the inflammation and granulation phases of healing, as clarified by the myofibroblast count. During plasma treatment, water may modify the wound surface through reducing the evaporative area, enhancing H<sub>2</sub>O<sub>2</sub> and nitrogen-based species, and

producing radiative warming. The histological stiffness of the wound surface during maturation and remodeling, however, may also influence the fate of such water.

### **Acknowledgments**

Nasruddin would like to acknowledge the help of the Directorate General of Higher Education (DIKTI), Indonesia, which supported him financially during his PhD study through the Joint Scholarship Program DIKTI-Kanazawa University, Japan. Part of this study was supported by JSPS KAKEN Grant Number 25293430 and 25390107 .

Keywords: cold plasma, plasma jet, wound healing, in vivo, myofibroblast

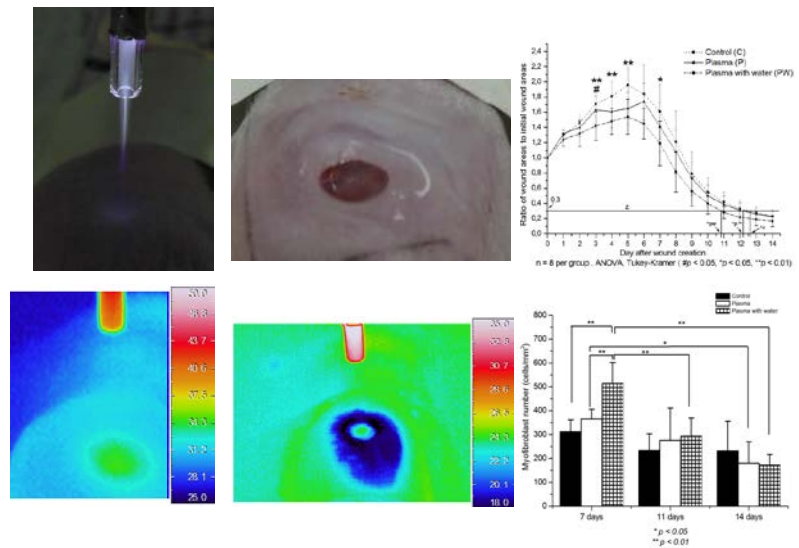
- [1]. G. Lloyd, G. Friedman, S. Jafri, G. Schultz, A. Fridman, K. Harding, *Plasma Process. Polym.* **2010**.7.194.
- [2]. K.-D. Weltmann, T.von Woedtke, *Eur. Phys. J. Appl. Phys.* **2011**. 55.13807.
- [3]. M. Laroussi, *IEEE Trans. on Plasma Sci.* **2009**.37.714
- [4]. E. Stoffels, *Contrib. Plasma Phys.* **2007**. 47.40.
- [5]. S. Baronski, A.Ayello E, Wound Care Essentials. 3rd ed. McKinney M, editor. Philadelphia: Wolters Kluwer & Lippincott Williams & Wilkins, **2012**
- [6]. V. Jones, JE. Grey, KG. Harding, *BMJ* 2006, 332, 777.
- [7]. M. Dyson, S. Young, CL. Pendle, DF. Webster, SM. Lang, *J. Invest. Dermatol.* **1988**.91.434.
- [8]. M. Dyson, S.R. Young, J.Hart, JA. Lynch, S. Lang, *J. Invest Dermatol.* **1992**.99.729
- [9]. MG. Kong, M.Keidar, K. Ostrikov, *J. of Physics D: Applied Physics.* **2011**. 44. 174018.

- [10]. T.v.Woedtke, H.-R.Metelmann, K.-D.Weltmann, *Contrib. Plasma Phys.* **2014**.54.104.
- [11]. MB. Witte MB, A. Barbul, *The Am. J. of Surgery.* **2002**. 183.406.
- [12]. A. Soneja, M. Drews, T. Malinski, *Pharmacol. Reports* **2005**. 57 Suppl:108
- [13]. AJ. Singer, RA. Clark, *N. Engl. J. Med.* **1999**. 341. 738
- [14]. A. Tanaka, T. Nakatani, J. Sugama, H. Sanada, A. Kitagawa, S. Tanaka, *EWMA.* **2004**. 4. 13.
- [15]. B. Hinz, SH. Phan, VJ. Thannickal, A. Galli, M-L. Bochaton-Piallat, G. Gabbiani, *The Am. J. of Pathol.* **2007**.170.1807.
- [16]. S. Roy, S. Khanna, A. Bickerstaff, SV. Subramanian, M. Atalay, M.Bierl, S. Pendyala, D. Levy, N.Sharma, M. Venojarvi, AR. Strauch, CG. Orosz, CK. Sen, *Circulation Res.* **2003**. 92.264.
- [17]. Nasruddin, Y.Nakajima, K.Mukai, HSE. Rahayu, M.Nur, T.Ishijima, H.Enomoto, Y.Uesugi, J.Sugama, T.Nakatani, *Clinical Plasma Medicine* **2014**. 2.28
- [18]. J. Heinlin, JL. Zimmermann, F. Zeman, W. Bunk, G. Isbary, M. Landthaler, T. Maisch, R. Monetti, G. Morfill, T. Shimizu, J. Steinbauer, W. Stolz, S. Karrer, *Wound Rep. Reg.* **2013**.21.800.
- [19]. R. Fernandez, R. Griffiths.*Cochrane Database of Systematic Reviews* **2012**, 2.
- [20]. M. Teschke, J. Kedzierski, E. Finantu-Dinu, D. Korzec, J. Engemann, *IEEE Trans. Plasma Sci.* **2005**.33.310.
- [21]. K.Ninomiya, T.Ishijima, M.Imamura, T.Yamahara, H.Enomoto, K.Takahashi, Y.Tanaka, Y.Uesugi, N.Shimizu, *J.Phys.D:Appl.Phys.* **2013**.46.425401
- [22]. WA. Armstrong , Facey R A, Grant D W, Humphreys W G, *Can. J. Chem* **1963**. 41.1575

- [23]. S. Kanazawa, H. Kawano, S. Watanabe, T. Furuki, S. Akamine, R. Ichiki, T. Ohkubo, M. Kocik, J. Mizeraczyk, *Plasma Sources Sci. Technol.* **2011**.20. 034010
- [24]. T. Sato, M. Yokoyama, K. Johkura, *J. Phys. D: Appl. Phys.* **2011**. 44. 372001
- [25]. G. Broughton II, J. E. Janis, C. E. Attinger, *Plast. Reconstr. Surg.* **2006**.117. Supplement 7.12S
- [26]. Z. Xia, A. Sato, M. A. Hughes, G. W. Cherry. *Wound Rep. Reg.* **2000**.8.138.
- [27]. O. Volotskova, M. A. Stepp, M. Keidar, *New J. Phys.* **2012**.14.053019
- [28]. S. Yonemori, R. Ono, *J. Phys. D: Appl. Phys.* **2014**.47.125401
- [29]. J. W. Flur, S. Sassning, O. Lademann, M. E. Darvin, S. Schanzer, A. Kramer, H. Richter, W. Sterry, J. Lademann, *Experimental Dermatology*. **2011**.21.130.
- [30]. P.-I. Brånemark, R. Ekholm, B. Albrektsson, J. Lindström, G. Lundborg, J. Lundskog, *J. Bone Joint. Surg. Am.* **1967**.49.48
- [31]. S. Roy, S. Khanna, K. Nallu, T. K. Hunt, C. K. Sen, *Molecular Therapy*. **2006**. 13. 211.

## Text for table of contents

A simple technique is tested to improve the contractile effect of cold plasma on wounds. Water is dropped on wounds before treatment. To evaluate its effect, macroscopic and immunohistological studies are performed. We show that combination treatment of plasma with water appeared to promote the wound contractile effect compared with plasma treatment alone. Plasma may modify wounds via water, chemically and physically. Wound maturation may also influence the fate of water during treatment.



**Keywords:** cold plasma, plasma jet, wound healing, in vivo, myofibroblast